Sensors & Transducers, Vol. 246, Issue 7, November 2020, pp. 1-8

www.sensorsportal.com

Sensors & Transducers

Published by IFSA Publishing, S. L., 2020
http://www.sensorsportal.com

Reconfigurable Sensor Based on PCB Technology for Moisture and Temperature Measurement

[1] A. dos Santos, [1] J. Monsalve-Diaz, [2] Pedro Carvalhaes-Dias, [3] F. Oliveira Morais, [1] P. Dias-Lima, [1] Fábio Serra Flosi and [1, *] J. A. Siqueira Dias

[1] University of Campinas, DSIF, Av. Albert Einstein, 400 - Campinas, SP, Brazil
[2] Universidade Tecnológica do Paraná, DAELE, Av. Alberto Carazai, 1640, C. Procópio, Brazil
[3] Universidade Júlio de Mesquita, Faculdade de Ciências e Engenharia,
R. D. Costa Lopes, 780, Tupã, SP, Brazil
[2] Tel.: 55 19 3521-4901
E-mail: siqueira@demic.fee.unicamp.br

Received: 21 September 2020 /Accepted: 22 October 2020 /Published: 30 November 2020

Abstract: A sensor that uses a modified fringing field capacitive sensor based on PCB technology to measure both capacitance and temperature is presented. The conventional interdigitated structure of the fingers in a capacitive fringing field sensor based on PCB technology is modified to allow its reconfiguration to measure both capacitance and temperature (using the copper tracks of the PCB as a Resistance Temperature Detector sensor). A sensor was fabricated and measurements of temperature and capacitance were taken in laboratory, using controlled amounts of water to cover the PCB surface. Since the sensor can measure temperature, it is possible to compensate for the variations of capacitance with temperature, a phenomena well described in the literature.

Keywords: Moisture sensor, Reconfigurable sensor, Capacitance measurements, Temperature measurements, PCB technology, Fringing field capacitor.

1. Capacitance Sensors

When a physical characteristic of a capacitor changes its structure due to an external agent, we obtain a capacitive sensor. Capacitive sensors structures are used for various applications. For example, if a physical parameter, like the permittivity of the dielectric or the distance between electrodes, changes, the capacitance of the structure changes, and the capacitance variation can be correlated to the physical parameter change.

One of the interesting features of such capacitive sensors is that the capacitor electrodes can be physically isolated from the sensing environment, as in the case of fringing field capacitive sensors.

In fringing field capacitive sensors, the material that is near the capacitor electrodes changes the dielectric of the capacitor, but no physical contact is required between the electrodes and the material that is over the electrodes. Capacitive fringing fields sensors are employed in various applications, and advanced irrigation management systems are among them [1-3]. Although there many techniques used to implement precise soil water content sensors for irrigation (based on heat transfer [4-6], tensiometric [7] and electrical resistance, capacitance [8-10] is a valuable technique for measuring soil water content.

Capacitance fringing field sensors based on PCB technology are also used for measuring moisture in several applications like cement [11], stored grains [12] and paper pulp [13, 14].

Another important feature of the capacitive fringing field sensors is that low-frequency signal processing circuits can be used to measure the capacitance. These systems are simple to design and operate, when compared to high-frequency RF interrogation systems.

Also, a simple PCB can be used to fabricate the capacitive sensor, resulting in an extremely low-cost sensor.

Conventional fringing field PCB capacitive sensor consists of a large number of interdigitated coplanar electrodes, as shown in Fig. 1.

We pattern, on a PCB, n copper tracks (called fingers) with thickness h, separated by a distance d and with a length l. The capacitance of the structure is given by:

$$C = \varepsilon_0 \varepsilon_r \frac{nlh}{d} \quad (1)$$

The value of the capacitance changes if a material with a different ϵ_r is placed in contact with the PCB surface. A typical example is irrigation water being applied in a soil, where the measured variations in the sensor's capacitance can be correlated with the amount of water in the soil.

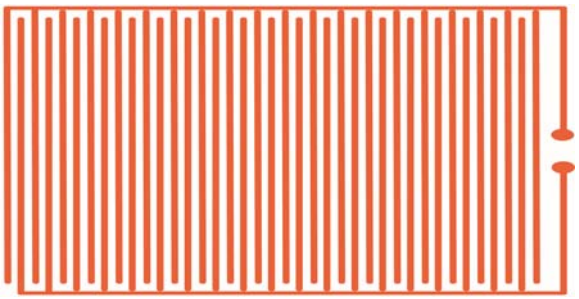


Fig. 1. Layout of a conventional PCB interdigitated capacitor.

This type of sensor has already been used to measure moisture and it has been shown that the capacitance of the PCB fringing field capacitors change with temperature [9]. Therefore, it is necessary to use another sensor (a temperature sensor) to measure the temperature and correct for the capacitance measurement.

In this work we present an application of the reconfigurable sensor based on PCB technology (presented in [16]) to measure moisture and temperature, allowing for the correction of the capacitance measurement as a function of the sensor's temperature.

2. The Modified Fringing Field Capacitor Structure

In Fig. 1 we present the conventional layout of the PCB fringing field capacitor, with interdigitated fingers. In a layout with n fingers, we have $n/2$ fingers connected to each of the contacts where the capacitance measurement is made.

The new pattern, proposed in [16], is made using two parallel long copper tracks, with a serpentine shape, as shown in Fig. 2.

Since the sensor will be used inserted into moisturized soils, to protect the PCB tracks a conventional solder mask was applied on both sides of the PCB to protect it.



Fig. 2. The layout of the reconfigurable sensor has two long parallel copper tracks instead of interdigitated fingers.

3. Measuring Capacitance and Temperature with the Reconfigurable Sensor

Using this new configuration, depending on which points we make contact with the PCB tracks, it is possible to make the conventional capacitance measurement, or measure the resistance of one of the continuous copper tracks.

Making contacts at the beginning (or end) of the two parallel tracks, we make the conventional measurement of capacitance, as shown in Fig. 3. If we make contacts at the beginning and at the end of any of the single continuous tracks, as shown in Fig. 4, we have a resistor composed of a long line of copper, and we can measure its resistance.



Fig. 3. Contact points for measuring capacitance in the novel PCB structure.

Since copper can be used to make resistance temperature detectors (RTD) [17-19], we can use this measurement of resistance to measure the sensor temperature.

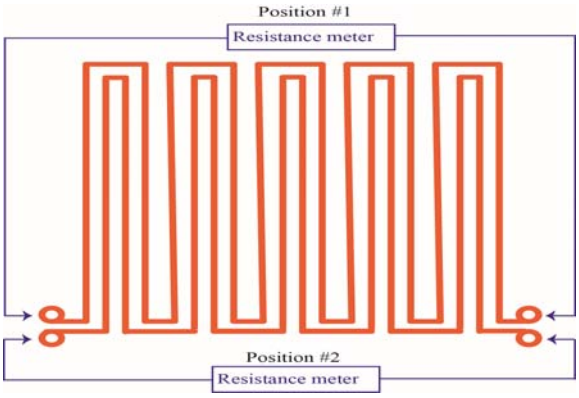


Fig. 4. Contact points for measuring resistance in the novel PCB structure.

4. Materials and Methods

4.1. The Reconfigurable Sensor

We fabricated a sensor using a FR-4 PCB with a thickness of 1.6 mm and measuring 96 mm × 94 mm. A photograph of the sensor is shown in Fig. 5.



Fig. 5. Photograph of the fabricated sensor.

4.2. Temperature Measurements using the Copper Tracks

Platinum and copper are metals usually used to fabricate RTDs. Copper has a very small TC, and the resistance *R(T)* of a copper wire can be written as:

$$R(T) = R_0[1 + \alpha(T - T_0)], \quad (2)$$

where R_0 is the value of the resistance at a temperature $T = T_0$, and $\alpha \approx 0.00420\ \Omega/\ ^oC$.

Using (2) we can calculate the variation of *R(T)* with temperature as:

$$\frac{dR(T)}{dT} = \alpha R_0 \quad (3)$$

In our PCB we measured the continuous track of copper R0 = 7.913 Ω (at T_0 = 25 ºC), what leads to

$$\frac{dR(T)}{dT} = 0.0332\Omega \quad ^oC \quad (4)$$

If we force a current I_0 = 10 mA in the resistance *R(T)* of the copper track, the voltage variation ΔV on it when submitted to a temperature variation of 1 ºC is only ΔV ≈ 332 μV.

Thus, we used a simple amplifier circuit to measure temperature using the PCB copper tracks. A basic block diagram of the circuit [16] is shown in Fig. 6, and the implemented circuit is presented in Fig. 7.

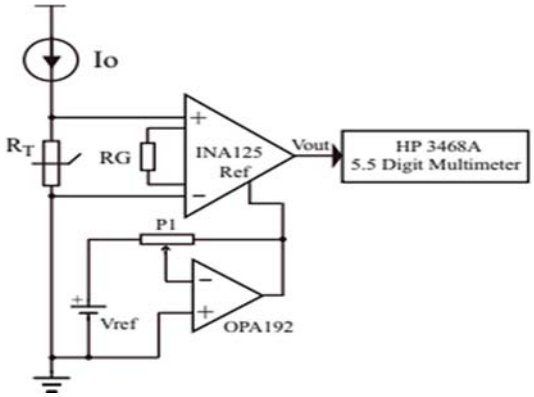


Fig. 6. Block diagram of the amplifier (with off-set adjust) used to measure temperature using the PCB copper tracks.

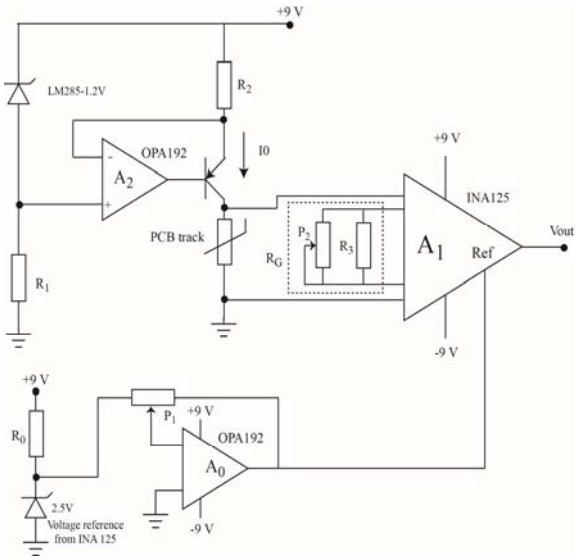


Fig. 7. Amplifier (with off-set adjust) used to measure temperature using the PCB copper tracks.

A current source I_0 = 10 mA was applied to the sensor. The voltage on R_T is sent to an INA125 instrumentation amplifier, adjusted with a gain G_V = 30.12, so that the output of the instrumentation amplifier has a slope *dVout /dT* ≈ 10 mV/ºC.

Since at T = 0 ºC the resistance of the copper track is not zero, there is an off-set at the output of the amplifier at this condition and, to cancel this off-set, we applied, to the INA 125 instrumentation amplifier, a negative voltage generated by the inverting amplifier implemented with op-mp A_0 (OPA192).

The current source I_0 is implemented with op-amp A_2, the voltage reference LM 285-1.2, resistor R_2 and PNP transistor *Q1*. Due to the negative feed-back, the voltage at the non-inverting input of A_2 appears at its inverting input. This forces the 1.2 V voltage at the LM285-1.2 to appear on R_2, so that the current that flows in R_2 is given by:

$$I_0 = \frac{1.2V}{R_2} \quad (5)$$

This current enters in the emitter of Q1, and neglecting the base current of Q1, we can consider that this current leaves the collector and bias the PCB tracks. With R_2 = 1.2 kΩ, the nominal value of I_0 is 10 mA.

The voltage on the copper resistor formed by the PCB tracks is amplified by the INA 125 instrumentation amplifier (from Texas Instruments, USA) with a gain given by:

$$G_V = 4 + \frac{60k\Omega}{R_G} \quad (6)$$

The value of RG (the equivalent of P_2 and R_1 connected in parallel) is adjusted to force the output voltage of A_1 to have a well-defined thermal behaviour, *Vout* = 10 mV/ºC.

A calibration of the circuit was performed using a, in the thermal chamber in the 9 ºC to 50 ºC temperature range. A temperature sensor (LM 135 from Texas Instruments, USA). The plot of the measured values of *Vout* as a function of the measured temperature with the LM 135 is shown in Fig. 8.

4.3. Capacitance Measurements

To measure the capacitance of the PCB fringing field capacitor, we used a simple relaxation oscillator, shown in Fig. 9.

From the measurements presented with this PCB fringing field capacitor presented in [16], we expect to measure a capacitance in the order of approximately 400 pF.

The circuit uses the TLV 3501 (Texas Instruments, USA), a fast (4.5 ns) rail-to-rail comparator. The developed circuit uses a reference voltage obtained by the resistor divider R_3-R_4, buffered by an OPA192 op-amp. Resistor R_0 = 102 kΩ, used to charge and discharge de PCB fringing field capacitor, was calculated to generate an oscillating frequency in the order of 22 kHz (a period T = 45 µs).

With this oscillating frequency, the rise and fall time of the comparator can be neglected since it is three orders of magnitude smaller that the period of the oscillating square wave.

The feed-back resistors that create the hysteresis are equal (R_1 = R_2 = 100 kΩ), creating a symmetrical charge and discharge signal around *Vdd/2*.

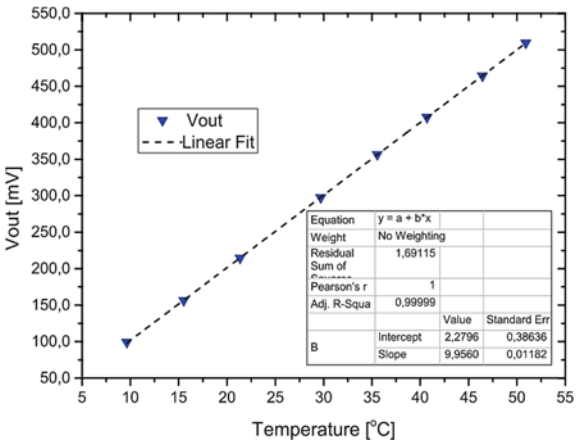


Fig. 8. Comparison of measured temperature with the LM 185 sensor and the value of *Vout* fabricated PCB sensor.

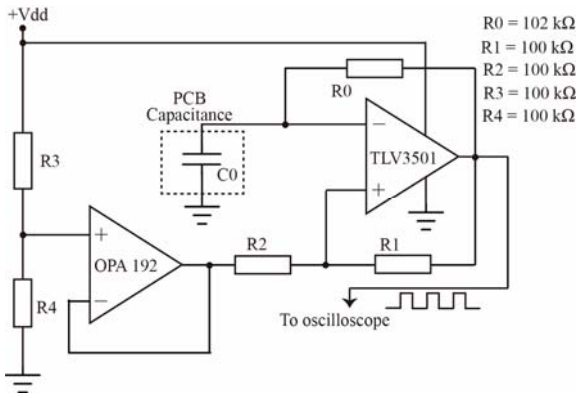


Fig. 9. Circuit of the relaxation oscillator.

The waveform of the charge/discharge of a 10 nF capacitor and of the comparator output are shown in Fig. 10.



Fig. 10. Measured waveform in the relaxation oscillator.

The relaxation oscillator of Fig. 9 has its oscillating frequency given by:

$$f_{osc} = \frac{1}{R_0 C_0 ln(3)} \quad (7)$$

Therefore, measuring the frequency f_{osc} we can calculate C_0:

$$C_0 = \frac{1}{R_0 f_{osc} ln(3)} \quad (8)$$

We performed a test with the relaxation oscillator. to check if it is possible to, using the oscillator output frequency measured with an oscilloscope, calculate C_0 using (8) with a good precision.

Firstly, we measured (with a Genrad 1659 RLC Digibridge) five commercial capacitors, in the 275.5 pF to 878.4 pF range. Next, we used these capacitors in the relaxation oscillator and measured its oscillating frequency with an oscilloscope.

The plot shown in Fig. 11 shows a comparison of the capacitors measured with the RLC bridge and with the relaxation oscillator. The linear fit shown in Fig. 11 has $R^2 = 0.99996$, showing that the capacitors measured with the relaxation oscillator agree very well with the measurements made with the RLC bridge.

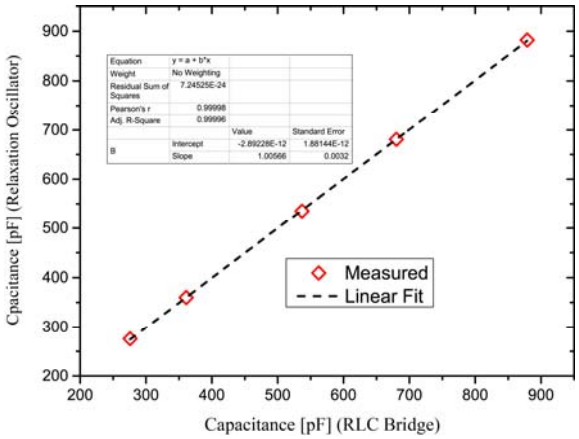


Fig. 11. Comparison of the capacitors measured with the Genrad 1659 RLC Digibridge and the developed relaxation oscillator.

4.4. Moisture and Temperature Measurements

A temperature sensor LM 185 (from Texas Instruments, USA) was protected with a thin silicone layer (applied by spray), so it can be in contact with water. The sensor was glued to the surface of the PCB sensor.

We cut three pieces of an absorbent paper (in squares with 3.0 cm × 3.0 cm). The pieces of paper were put on a scale, and we wet each piece of paper with the same amount of water (0.13 g).

The PCB sensor was put in a thermal chamber, and the oscillator output frequency was measured with an oscilloscope, as we add, one by one, the pieces of paper to the PCB surface. Special attention was given to the placement of the pieces of paper on the sensor surface, avoiding any overlapping between papers.

A photograph of the sensor with 3 pieces of wet paper on its surface is shown in Fig. 12.

These measurements of frequency were repeated (with one, two and three pieces of paper on the sensor surface), at two temperatures: at 20 °C and 30 °C. The temperature was measured with the LM 185.

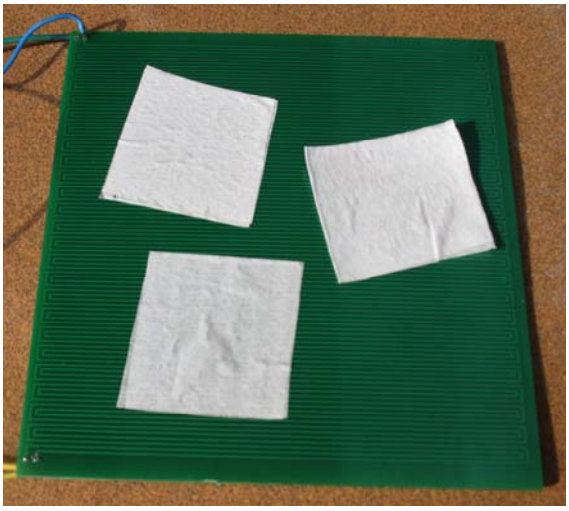


Fig. 12. Set-up used to measure capacitance as a function of the water mass.

5. Results

5.1. Temperature Measurements

In Fig. 13 we have a plot comparing the measured temperatures with the fabricated sensor (using the PCB tracks) and the LM 185.

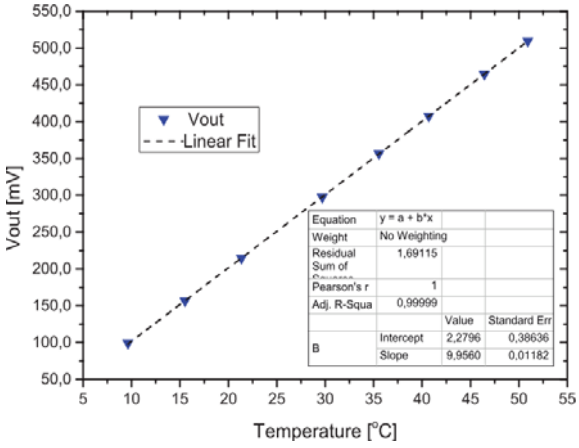


Fig. 13. Comparison of measured temperature with the LM 185 sensor and the value of V_{out} measured with the fabricated PCB sensor.

In Table 1 we present the errors between the measured values (*Vout*) and the calculated value of *T* using the linear fit shown in Fig. 13, considering that $dVout/dT \approx 10$ mV/ºC.

As it can be observed, the error *E* between the measured values using the LM 185 and the PCB tracks is $E \leq 0.14$ ºC.

It is worth noting that a small change in the off-set adjustment of the amplifier circuit (in the negative direction) would lead to an even better agreement between the measured data with the LM 185 and the developed sensor.

Table 1. Temperature measurements

Temperature		
LM185	**PCB sensor**	**Error**
20 ºC	20.14 ºC	0.14 ºC
25 ºC	25.12 ºC	0.12 ºC
30 ºC	30.09 ºC	0.09 ºC

5.2. Moisture Measurements

In Fig. 14 and Fig. 15 we present plots of the measured capacitance, as a function of the mass of water covering the PCB, for $T = 20$ and $T = 30$ ºC.

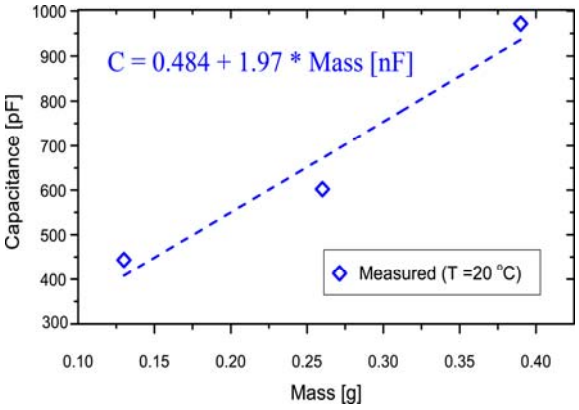


Fig. 14. Measured capacitance as a function of the water mass on the surface of the sensor, at T = 20 ºC.

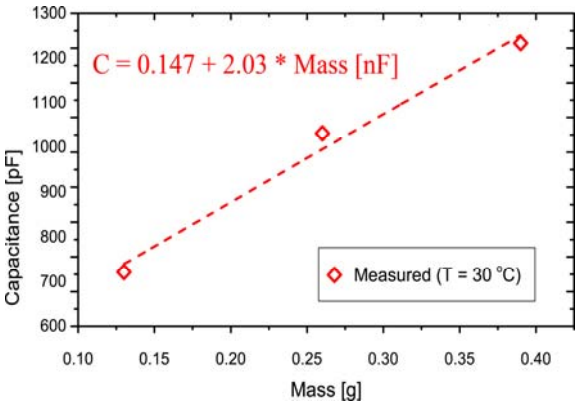


Fig. 15. Measured capacitance as a function of the water mass on the surface of the sensor, at T = 30 ºC.

As expected, we observed, for the same water mass, a variation of the measured capacitance depending on the sensor temperature.

As we can notice, both curves have approximately the same slope (as we can see in the plot of Fig. 16, where both curves are plotted together), indicating that in this small mass of water range we can consider that the capacitance varies linearly as a function of the mass.

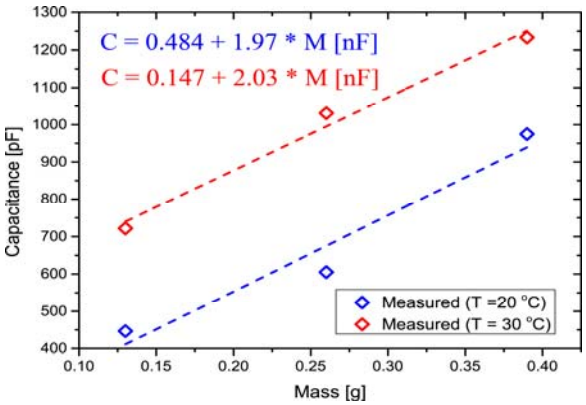


Fig. 16. Measured capacitance as a function of the water mass on the surface of the sensor, at T = 30 ºC.

Therefore, we can calculate a compensation equations, using the two straight line equations presented in Fig. 16:

$$C = 0.147 + 2.03Mass, \quad (9)$$

$$C = 0.484 + 1.97Mass, \quad (10)$$

where the variable *Mass* is the mass of water (in grams) and the capacitance *C* is given in nF.

Since (9) and (10) have approximately the same slope, we can obtain a set of equations that cover all parallel straight lines between these line equations, with *k* as a parameter:

$$C = k + 2.0Mass \quad (11)$$

In (9) we used an average slope value of $m = 2$ nF/g and the capacitance is given in nF.

The value of *k* can be written as a linear function of the temperature, and since we have two points (*k,T*) in this straight line equation (*0.147,20*) and (*0.484,30*), we obtain:

$$k = -0.527 + 0.0337T \quad (12)$$

Thus, it becomes possible to correct the capacitance measurements, depending on the measured temperature, and obtain a reliable estimation of the water content on the PCB surface. Combining (8), (11) and (12) we can write:

$$Mass = \frac{1}{2}\left[\frac{1}{R_0 f_{osc} ln(3)} + 0.527 - 0.0337T\right] \quad (13)$$

Although in this work we have equations to correct for the capacitance only between T = 20 ºC to T = 30 ºC, with proper calibration it is easy to obtain equations to calculate the correct values of capacitance for any temperature.

6. Conclusions

A reconfigurable PCB sensor based on a modified structure of a fringing field capacitor was presented. A novel layout for the PCB capacitor fringing field was used, with two long parallel tracks instead of interdigitated electrodes.

Using this structure, if we change the contact points on the copper tracks, it is possible to measure both capacitance and temperature. Since the capacitance measured with a PCB fringing field structure depends on temperature and the dielectric constant of water also changes with temperature, by measuring the temperature of the material which is in contact with the PCB sensor (water, in our case) we can compensate for these variations and obtain a much better estimation of the moisture, using the compensation equations presented.

We demonstrated that a simple relaxation oscillator can be used to measure the capacitance of the PCB fringing field capacitor. The relaxation oscillator was characterized and a good agreement between the measured capacitance with the relaxation oscillator and a commercial RLC bridge was obtained. The fit line of the measured capacitance, in the 275.5 pF to 878.4 pF range, presented R^2 = 0.9994.

The sensor is extremely low-cost (only a conventional FR-4 PCB is required to fabricate it) and the signal processing circuits are also very simple. If we incorporated to the signal processing circuit a low-cost microcontroller (with an A/D converter), it is possible to measure the oscillator frequency (capacitance) and the resistance of the copper tracks (temperature).

Thus, a complete low-cost moisture sensor system can be easily implemented using the reconfigurable PCB sensor presented.

References

[1]. M. Bittelli, Measuring Soil Water Potential for Water Management in Agriculture: A Review, *Sustainability,* Vol. 2, Issue 5, 2010, pp. 1226-1251.

[2]. X. Dong, C. Vuran, S. Irmak, Autonomous, precision agriculture through integration of wireless sensor networks with center pivot irrigation systems, *Ad Hoc Networks,* Vol. 11, Issue 7, 2015, 1975–1987.

[3]. T. A. Brase, Precision Agriculture; *Thomson Delmar Learning*, New York, NY, USA, 2006.

[4]. M. França, F. Morais, P. Carvalhaes-Dias, L. Duarte, J. Siqueira Dias, A Multiprobe Heat Pulse Sensor for Soil Moisture Measurement Based on PCB Technology. *IEEE Transactions on Instrumentation and Measurement*, Vol. 68, Issue 2, 2019, pp. 606-613.

[5]. P. Carvalhaes-Dias, F. Morais, L. Duarte, A. Cabot, J. Siqueira Dias, Autonomous Soil Water Content Sensors Based on Bipolar Transistors Encapsulated in Porous Ceramic Blocks, *Applied Sciences*, Vol. 9, Issue 6, 2019, 1211.

[6]. L. Matile, R. Berger, D. Wachter, R. Krebs, Characterization of a New Heat Dissipation Matric Potential Sensor, *Sensors*, Vol. 13, Issue 1, 2013, pp. 1137-1145.

[7]. B. Hanson, D. Peters, S. Orloff, Effectiveness of tensiometers and electrical resistance sensors varies with soil conditions, *California Agriculture*, Vol. 54, Issue 3, 2000, pp. 47-50.

[8]. E. Ferreira da Costa, N. E. de Oliveira, F. Morais, P. Carvalhaes-Dias, L. C. Duarte, A. Cabot, A Self-Powered and autonomous fringing field capacitive sensor integrated into a micro sprinkler spinner to measure soil water content, *Sensors*, Vol. 17, Issue 3, 2017, 575.

[9]. R. N. Dean, A. K. Rane, M. E. Baginski, J. Richard, Z. Hartzog, D. J. Elton, A capacitive fringing field sensor design for moisture measurement based on printed circuit board technology, *IEEE Transactions on Instrumentation and Measurement*, Vol. 61, Issue 4, 2012, pp. 1105–1112.

[10]. H. Elle, A. Denoth, A capacitive soil moisture sensor, *Journal of Hydrology*, Vol. 185, Issue 1, 1996, pp. 137–146.

[11]. M. N. Alam, R. H. Bhuiyan, R. A. Dougal, M. Ali, Concrete moisture content measurement using interdigitated near-field sensors, *IEEE Sensors Journal*, Vol. 10, Issue 7, Jul. 2010, pp. 1243-1248.

[12]. R. N. Dean, J. D. Craven, E. A. Guertal, K. A. Varnavas, PCB Sensor for status monitoring of stored food stocks, *IEEE Sensors Letters*, Vol. 3, Issue 4, 2019, pp. 1–4.

[13]. K. Sundara-Rajan, L. Bryd II, A. V. Mamishev, Moisture content estimation in paper pulp using fringing field impedance spectroscopy, *IEEE Sensors Journal*, Vol. 4, Issue 3, Jun. 2004, pp. 378–383.

[14]. F. Morais, P. Carvalhaes-Dias, L. Duarte, E. Costa, A. Ferreira, J. Siqueira Dias, Fringing Field Capacitive Smart Sensor Based on PCB Technology for Measuring Water Content in Paper Pulp, *Hindawi Journal of Sensors*, Vol. 2020, 2020, Article ID 3905804.

[15]. A. Chanzy, J.-C. Gaudu, O. Marloie, Correcting the Temperature Influence on Soil Capacitance Sensors Using Diurnal Temperature and Water Content Cycles, *Sensors,* Vol. 12, Issue 7, 2012, pp. 9773-9790.

[16]. P. Carvalhaes-Dias, J. Monsalve-Diaz, F. Morais, A. dos Santos, P. Dias-Lima, J. A. Siqueira Dias, Proposal of a Reconfigurable Sensor for Measuring Temperature and Capacitance, in *Proceedings of the 6th International Conference on Sensors Engineering and Electronics Instrumentation Advances (SEIA'2020)*, Porto, Portugal, 23-25 September 2020, pp. 18-20.

[17]. R. H. Marsh, Selecting Thermocouples and Platinum Resistance Temperature Detectors, *Journal of Control Engineering*, Vol. 18, Issue 11, November 1971, pp. 76-77.

[18]. P. Carvalhaes-Dias, I. P. Ferreira, F. J. Oliveira Morais, L. F. Caparroz Duarte, J. A. Siqueira Dias, Analog Linearization of Resistance Temperature Detectors (RTD) Using the Intrinsic Curvature of BandGap Voltage References, in *Proceedings of the 4th International Conference on Sensors Engineering*

and Electronics Instrumentation Advances (SEIA'18), Amsterdam, The Netherlands, 19-21 September 2018, pp. 68-71.

[19]. P. Carvalhaes-Dias, I. P. Ferreira, L. C. Duarte, Flávio J. O. Morais, J. A. Siqueira Dias, Using the Non-linear Behavior of the Brokaw Bandgap Voltage Reference Cell to Linearize Resistance Temperature Detectors (RTD), *Sensors & Transducers*, Vol. 229, Issue 1, January 2019, pp. 61-67.

Published by International Frequency Sensor Association (IFSA) Publishing, S. L., 2020 (http://www.sensorsportal.com).

